

Optical brake induced by laser shock waves

Qiao Kang*, Dongyi Shen*, Jie Sun*, Xin Luo[†], Wei Liu*, Zhihao Zhou[†],
Yong Zhang[‡] and Wenjie Wan^{*,†,§}

**The State Key Laboratory of Advanced Optical
Communication Systems and Networks, School of Physics and Astronomy,
Shanghai Jiao Tong University, Shanghai 200240, P. R. China*

*†MOE Key Laboratory for Laser Plasmas and
Collaborative Innovation Center of IFSA,
University of Michigan-Shanghai Jiao Tong University Joint Institute,
Shanghai Jiao Tong University, Shanghai 200240, P. R. China*

*‡National Laboratory of Solid State Microstructures,
College of Engineering and Applied Sciences, Nanjing University,
Nanjing 210093, P. R. China
§wenjie.wan@sjtu.edu.cn*

Received 14 May 2021

Revised 28 May 2021

Accepted 30 May 2021

Published 26 July 2021

We demonstrate an optical method to modify friction forces between two close-contact surfaces through laser-induced shock waves, which can strongly enhance surface friction forces in a sandwiched confinement with/without lubricant, due to the increase of pressure arising from excited shock waves. Such enhanced friction can even lead to a rotating rotor's braking effect. Meanwhile, this shock wave-modified friction force is found to decrease under a free-standing configuration. This technique of optically controllable friction may pave the way for applications in optical levitation, transportation, and microfluidics.

Keywords: Nonlinear optics; laser plasma; shockwave; friction.

1. Introduction

Lasers have become a powerful and convenient tool for micro/nanoparticle manipulations, enabling optical tweezers,¹ trapping,^{2,3} levitation,⁴ and optical atom cooling,⁵ where the radiation pressure of laser can exert forces upon sub-microscopic objects like atoms,⁵ cells,⁶ molecules,⁷ bacteria and viruses,¹ and droplets.⁸ Such laser-enabled optical manipulation methods benefit from the noninvasive feature, remote control, and high accuracy, enabling a wide range of applications in biomedicine, physics science, and nanotechnology. The profound development of a high-power laser has further pushed the limit of laser manipulation into macroscopic

§Corresponding author.

scale, allowing high-power laser interactions with macroscopic objects. This technological leap for high-power lasers has led to intriguing applications such as laser propulsion,^{9–12} laser peening,^{13–15} laser cleaning,^{16,17} laser adhesion test,¹⁸ laser processing and fabrication,^{19–21} where high-power lasers bring up precision and new functionalities into these traditional industry branches. Many of these techniques are associated with laser-induced shock wave generations, which are frequently encountered phenomena when high-power lasers interact with matters.²² The strong absorption of incoming laser pulses can directly induce sudden ionization and vaporization of the target materials, simultaneously generating high-density and high-temperature plasma.²³ As a result, the quick thermal dynamical expansion of such laser plasma triggers the generation of shock waves with high pressure and density,²⁴ a crucial step for interaction with macroscopic objects like in laser propulsion and laser surface cleaning processes in the free space.^{10,16} On the other hand, the internal shock waves can penetrate into the target in a similar manner along with a high-pressure wave propagation, which can strengthen the materials internally in the laser peening application.¹³ Besides, studies of laser-induced shock waves are also investigated, where lasers meet two objects at their interface, for instance laser shock peening in the confined situation.²⁵

Two contacted objects generate resisting friction force, proportional to the normal pressure between the two objects, i.e., the famous Amontons' laws.²⁶ This is one of the oldest problems but with high importance in many areas like transportation,²⁷ fluid dynamics,²⁸ and aerodynamics.²⁹ The recent development of micro/nanotechnology has advanced this field into the microscopic regime, i.e., the science of tribology,³⁰ where the microscopic origin, for example, interatomic bonds and nanoscale roughness,³¹ for such interface, friction is still under debate, but prior studies have shown the possibility for optically controlled friction or fluid viscosity through photoinduced state change at the molecular level.³² But at the macroscopic level, there has not been much process for reducing friction, except the focus on lubrication studies.³³ One interesting solution using ultrasonic vibration has shown a potential for friction reduction, given the idea of reduced contact areas.^{34,35} Inspired by all of these works, we are interested in the problem of laser-modified friction at the interface.

Here, we experimentally demonstrate optical modification to surface friction through laser shock waves, which are induced by the excitation of laser plasma between two contacted surfaces. A strong enhancement of such friction forces can be realized in a sandwiched confinement owing to the increase of pressure deriving from excited shock waves. The enhanced friction increases with the input laser power, which can be further increased to “brake” a rotating motor. Similar dynamics have also been observed, but with less efficiency, in the presence of lubricants. Moreover, under the configuration of two free-standing objects, a reduction of friction is observed instead due to the decreased contact caused by pressured shock waves at the interface. This technique of optically controllable friction may pave way for critical areas like levitated hyperloop transportation³⁶ in the macroscopic scale and also for microfluidics application.³⁷

2. Principle

An intense pulsed laser focuses on a solid target's surface, e.g., metal, which leads to a rapid temperature increase at the focal spot. The accumulated heat can finally lead to ionization and vaporization of the material in the form of high-temperature and high-pressure plasma.²³ Consequently, plasma expansion further escalates into shock wave generation,²⁴ containing both high density and high pressure in the wavefront. In the experiment, metallic material is always chosen to generate shock waves for its small ionization energy. While for other materials, shock waves can also be generated by the ionization of air surrounding the target. Previously, such shock waves have enabled many intriguing applications like laser propulsion and laser cleaning,^{10,16} but, mainly in free space. However, it has also been shown that a structure with confined geometry can further enhance internal pressure P induced by such laser shock waves as the confined configuration retards plasma expansion, meanwhile, extends the interaction time between the laser shock and the target.³⁸ For example, laser peening through shock wave generations can induce compressive residual stresses to materials, enhancing fatigue resistance of materials.¹³

Inspired by these works, we are interested in the laser shock wave at the interface between two solid objects, especially on their effect to surface friction. As shown in Fig. 1, in our experiment, an intense pulsed laser is focused onto a metallic target through a transparent glass plate at their interface, where the shock wave can be excited with sufficient input power. The induced shock waves are well-confined internally as the metallic target is in close contact with the glass plate. As a result, this laser shock wave-induced pressure on the target can be greatly enhanced in the confined situation, and the pressure of the shock wave can be expressed as³⁹

$$P = 0.01 \times \left(\frac{\alpha}{\alpha + 3} ZI \right)^{1/2}, \quad (2.1)$$

where α indicates the fraction of plasma internal energy devoted to thermal energy, Z indicates the reduced shock impedance between the glass and the target, and I

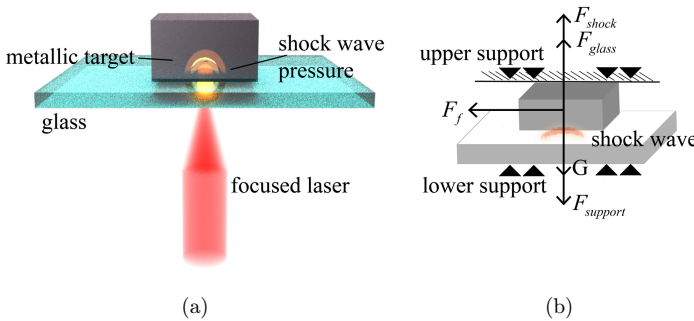


Fig. 1. (a) The schematics of the laser shock wave-induced pressure on the surface of the two close-contact targets. (b) Friction increases due to the increase of pressure drawing from shock waves under clamped configuration.

indicates laser intensity. α is considered as constant for the laser with a certain wavelength.⁴⁰ Z is dependent on the material of the target and confinement layer.⁴¹ As a result, the pressure can be modulated by laser intensity.

Consequently, this laser shock wave-induced pressure can increase the contact force normal to the surface between the two objects as shown in Fig. 1(b), this effect can be further enhanced when the shock waves penetrate the solids predicted by prior work.¹³ When the target is sliding on the glass, friction force resists the relative motion. Since shock wave pressure can increase the normal force, the surface friction force is expected to be altered by the new additional force F_{shock} . According to Amonton-Coulomb's law, the friction on the target can be expressed as

$$F_f = \mu(F_{\text{glass}} + F_{\text{shock}}) = \mu(F_{\text{glass}} + P \cdot s), \quad (2.2)$$

where μ represents the friction coefficient, μF_{glass} is the original friction between the metal and the glass plate, μF_{shock} indicates the additional friction induced by laser shock waves, P is a pressure term associated with the laser shock wave, while s is a stress area. Since the pressure of shock wave follows a Gaussian spatial distribution, the radius of stress area is usually considered as $\sqrt{2}$ times of the laser spot radius,⁴² which is about $100 \mu\text{m}$ in our experiment. Note that both the metal and the glass plate are externally clamped by solid supports to ensure a constant contact force F_{glass} , this allows the investigation of shock wave-induced pressure and the friction variation.

3. Results and Discussion

3.1. Laser-induced friction increase in a clamped configuration

In our experiment (Fig. 2(a)), a rotating metal rotor mounted on a DC motor is placed in close contact with a transparent glass plate, which allows an intense pulsed laser to be focused onto the contacting regime for shock wave generation. The rotor is made of steel, with width of 1 mm, outer diameter of 3 mm, and inner diameter of 1 mm. Here, a 1064 nm Nd:YAG laser with 8 ns pulse length and 10 kHz repetition rate has been used, while its power is varied for controlling the shock waves. The shock wave-induced pressure enhances the friction force onto the metal rotor causing a rising internal electrical current inside the DC-powered circuit. Experimentally, we can measure such changes by reading out the voltage variation across an inter-circuit resistor ($R = 20\Omega$). As the friction force exerted on the motor increases, the voltage rises along with the driving current. In this way, the dynamics of friction force between the rotor and the glass can be monitored, precisely. Using an oscilloscope, the temporal evolution of voltage due to laser-induced shock waves can be obtained to read out the change of friction.

Figure 2(b) shows the dynamics of driving voltage before/after introducing laser shock waves under the two scenarios with/without lubricants. When the metal rotor is irradiated by the pulsed laser, the voltages rise and stabilize at a larger constant value within several seconds, indicating an increase of friction at the interface.

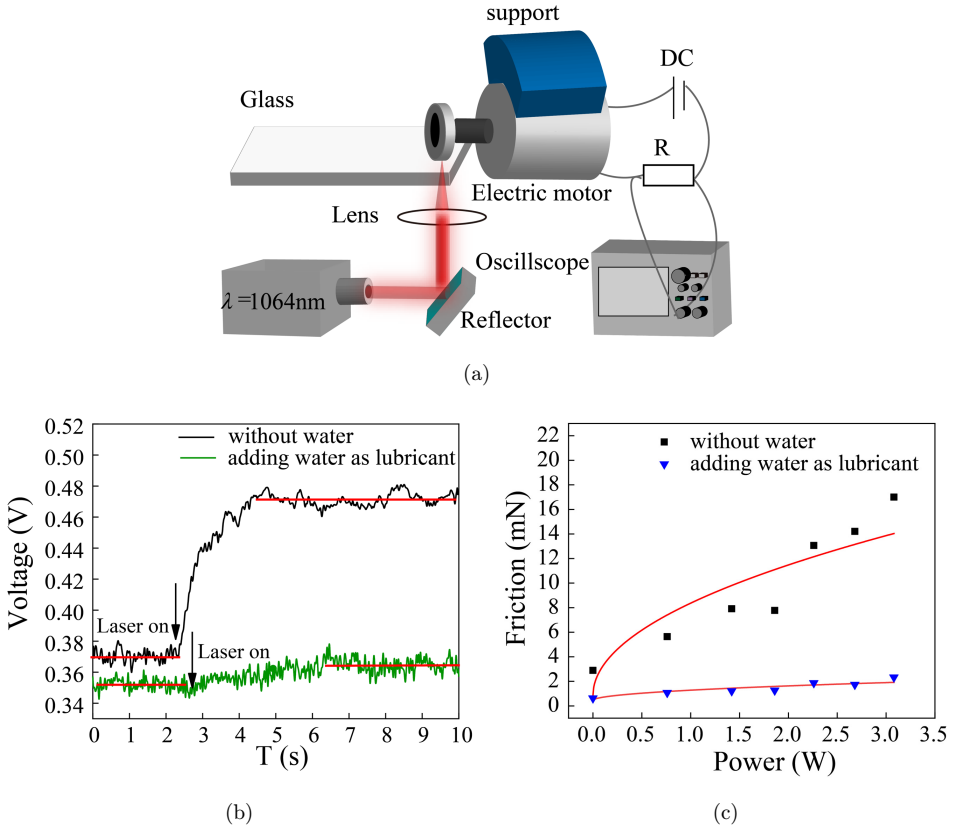


Fig. 2. (Color online) (a) The experimental setup of friction increase induced by the laser shock wave. (b) The voltage increases and stabilizes at a larger constant after turning on a laser with the power of 3.72 W. The green line and black line indicate voltage change in the situation with/without water lubricants, respectively. (c) The friction increases monotonically with the laser power.

Besides, after turning off the laser, the voltages decrease and stabilize at the initial value. Even for the case with a lubricant, i.e., water, noticeable changes have also been observed but much weaker than the former one without lubricants. Note that the initial voltage level with lubricant is lower than that without lubricant, indicating the reduction of friction due to the lubricant and the validity of the current method.

To be more precise, we explore the friction force variation under different laser powers. As shown in Fig. 2(c), the friction force increases gradually with the laser power. The red line is the theoretical line predicted by Eq. (2.1), which shows the friction force increases as $\text{power}^{1/2}$. The deviation between the red line and experimental data may be explained by the variation of surface condition during different tests. Here, the friction force is calibrated by the voltage reading and a force meter in a separated experiment, where the friction force is measured by the force meter. As the friction force exerted on the motor increases, the voltage increases accordingly.

Recording the friction force and the voltage simultaneously, the friction's one-to-one correspondence to the voltage variation can be set-up. As the laser power increases from 0.76 W to 3.08 W, the friction force rises from 5.6 mN to 17.0 mN without lubricant. In comparison, the lubricated case only shows an increase from 1.1 mN to 2.3 mN, much smaller than the dry case. Clearly, this effect of friction enhancement induced by laser shock waves has been weakened in the case with lubricant. This can be understood from the friction coefficient μ in Eq. (2.2), which is supposed to reduce under the presence of externally added lubricants. As a result, both the initial laser-off friction and the slope of friction increase when tuning up the laser is smaller in the lubricated case, as shown in Fig. 2(b).

3.2. Laser-induced optical braking

Moreover, such an increase of laser-induced friction forces can further lead to the stop of the rotating rotor, namely, "optical brake". Here, the driving force from the DC motor reaches the balance with the total friction, i.e., $F_{\text{drive}} = \mu(F_{\text{glass}} + F_{\text{shock}})$, we can expect the optical brake when the induced shock wave force exceeds this balance. Under a constant driving condition, i.e., fixed DC motor voltage at 0.4 V, an incident laser with 2.68 W power can brake the rotor within a second as shown in Fig. 3(b), where the initial contact friction force, i.e., μF_{glass} is calibrated to be 9.5 mN. Experimentally, this brake phenomenon can be visualized by observing the black paint on the motor's axle in Fig. 3(a). To monitor the brake phenomenon clearly, half of the axle is painted black. When the motor is rotating, the paint on the rotating axle turns blurry and indistinguishable, once the motor is braked by the laser-induced shock wave, the black paint on the axle becomes visible again. Furthermore, the initial friction force can be varied through adjusting the initial contact force, i.e., F_{glass} , in this manner, the inverse dependence of the two force components in Eq. (2.2) can be explored under the constant driving force. Figure 3(c) shows the relationship between the required laser power for optical brake and the initial friction force: the larger the initial friction is, the less power is required to realize optical brake, which is consistent with the theory predicted by Eq. (2.2). Combining Eqs. (2.1) and (2.2), we can express the laser power needed to brake the motor as $\text{Power} \sim (\mu F_{\text{glass}} - F_{\text{drive}})^2$, where μF_{glass} is the initial friction force. This dependence is fitted by the red line in Fig. 3(c).

3.3. Laser-induced friction decrease in a free-standing configuration

Surprisingly, this laser-induced shock wave can also suppress the friction force under an unclamped configuration in sharp contrast to the previous case. Here, if the original supporting stand on the top of the rotor is removed, we find that the final friction force settles down to a lower level compared to the initial one (Fig. 4(c)). In this configuration (Figs. 4(a) and 4(b)), the external support of the rotor no longer provides the balanced force against F_{glass} , F_{shock} , as a result, the contact force F_{glass} cannot be treated as a constant like in the former case. Moreover, when the shock

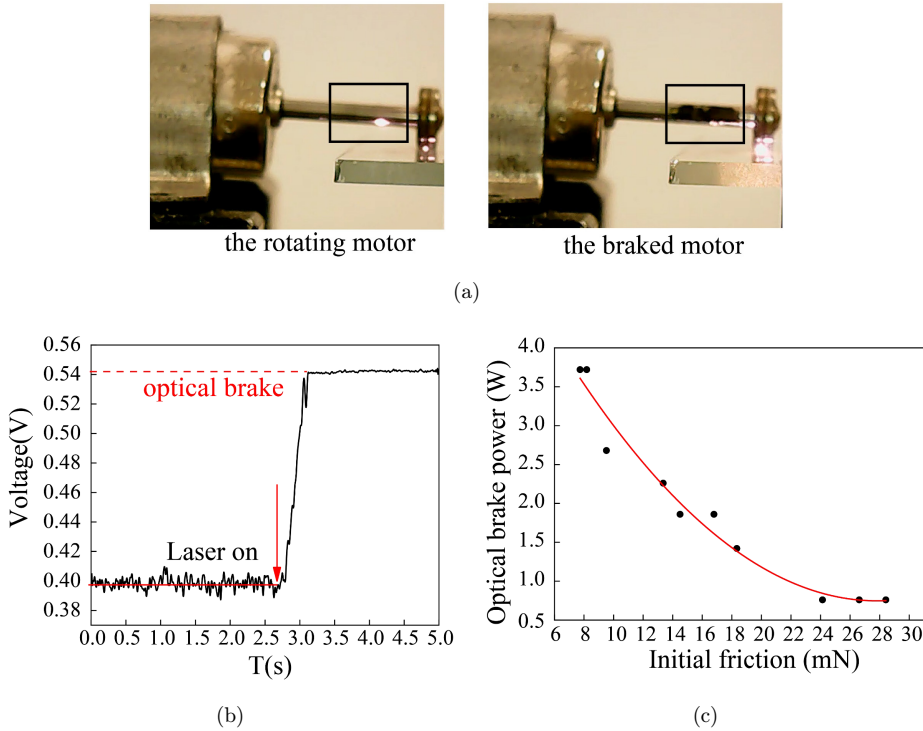


Fig. 3. (a) The rotating motor is braked by the laser which can be visualized by observing the black point on the axle. (b) “Optical brake” is realized within a second under the condition of 2.68 W laser power and 9.5 mN initial contact friction. (c) The required laser power for braking reduces when increasing the initial contact friction force.

wave force is strong enough to lift up the rotor, this action can introduce a separation gap between the rotor and the glass, reducing the contact area, much like the case using acoustic wave-induced friction reduction.^{34,35} The gap between the rotor and the glass can act as an air cushion, which dramatically reduces the friction coefficient μ . In an ideal case, the air gap should totally reduce the solid-contact friction down to zero. However, due to the pulsed scenario for the laser, the gravity can bring down the rotor right after the breakout, so that we may expect a temporal-averaged effect of friction reduction with the input laser power.

Figure 4(c) shows the temporal trace of the friction force through the driving voltage during a laser turn-on process. The voltage rapidly rises at first and quickly falls back, settling down to a stable level, when turning on a laser up to 1.42 W. Here, the spike may be explained by a similar argument like the previous clamped case when the rotor is still in close contact with the glass before the breakout. At first, the rotor is not lifted by the shock wave, and the shock wave can also enhance the contact force. While after a very short period of time, the oscillations of shock waves induce the separation between the rotor and the glass. And the final friction is

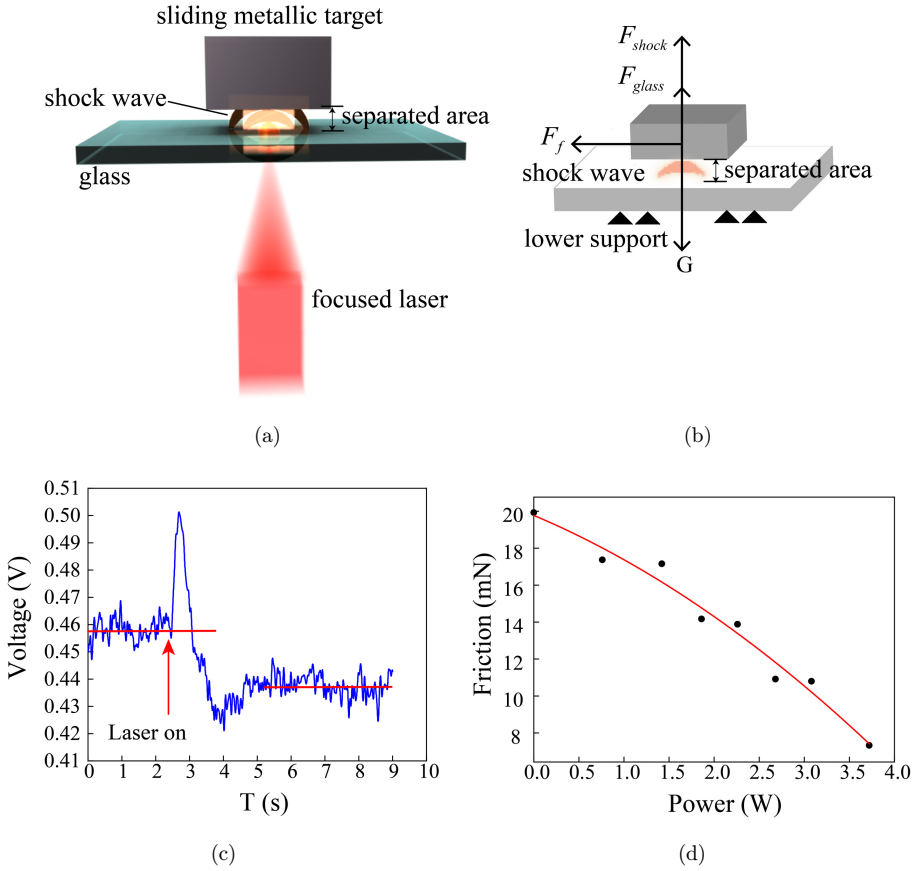


Fig. 4. (a) The schematics of shock wave-induced separation between contacted surfaces. (b) Friction declines for the reduction of contact area under an unclamped configuration. (c) The voltage drops and stabilizes at a lower value after turning on the laser with the power of 1.42 W. (d) The friction reduces with increasing laser power.

reduced due to the separation action. We record the stable voltage drop during the laser turn-on process and measure the reduced friction when varying input laser powers. As the power of the laser increases from 0.76 W to 3.72 W, the friction decreases from 17.4 mN to 7.3 mN as shown in Fig. 4(d). The friction force has dropped by half from the initial value (without laser) when the input laser reaches around 3.72 W. We believe the friction force can also be reduced to zero, i.e., achieving levitation⁴ if enough laser power can be supplied, which requires further investigation.

This demonstrated technique of controlling friction by laser-induced shock waves may have wide applications. Compared with traditional ways to control friction, this method is more flexible and well regulated by input laser power. This may offer an alternative way for modifying friction properties besides the lubricant approach.

With the advantages of tunability and precision, we envision that the method of optically controllable friction may have practical applications in critical areas, for example, in levitated hyperloop transportation,³⁶ instead of using the magnetic repulsion to levitate and propel trains, the optical technique provides a potential method to control friction between trains and tracks if high-power laser technology is mature in future. In microfluidics,³⁷ where the fluid viscosity can be considered as internal friction force generated between adjacent layers of fluid in relative motion, our technique of optically controllable friction may be also useful in manipulating microfluidics, while the traditional methods controlling fluid viscosity lay on the temperature control or the surface structure of microchannel.

4. Conclusion

In conclusion, we have demonstrated an optical technique to modify surface friction by laser-induced shock waves. The increase of surface friction can be realized through the induced pressure from laser shock waves in a sandwiched configuration. The enhanced friction increases monotonically with laser power and finally leads to an optical brake to a rotating rotor. On the other hand, under the condition of two free-standing objects, friction reduction is observed instead. This optical friction controlling method may be applicable for practical applications, such as levitated hyperloop transportation³⁶ and microfluidics.³⁷

Acknowledgments

This work was supported by the National Key Research and Development Program (Grant Nos. 2016YFA0302500 and 2017YFA0303700); National Science Foundation of China (Grant Nos. 92050113 and 11674228). Shanghai MEC Scientific Innovation Program (Grant No. E00075).

References

1. A. Ashkin and J. M. Dziedzic, Optical trapping and manipulation of viruses and bacteria, *Science* **235** (1987) 1517–1520.
2. L. Chen, W. Liu, D. Shen, Y. Liu, Z. Zhou, X. Liang and W. Wan, All-optical tunable plasmonic nano-aggregations for surface-enhanced Raman scattering, *Nanoscale* **11** (2019) 13558–13566.
3. O. M. Maragò, P. H. Jones, P. G. Gucciardi, G. Volpe and A. C. Ferrari, Optical trapping and manipulation of nanostructures, *Nat. Nanotechnol.* **8** (2013) 807.
4. A. Ashkin and J. Dziedzic, Optical levitation by radiation pressure, *Appl. Phys. Lett.* **19** (1971) 283–285.
5. S. Chu, L. Hollberg, J. E. Bjorkholm, A. Cable and A. Ashkin, Three-dimensional viscous confinement and cooling of atoms by resonance radiation pressure, *Phys. Rev. Lett.* **55** (1985) 48.
6. K. Dholakia, P. Reece and M. Gu, Optical micromanipulation, *Chem. Soc. Rev.* **37** (2008) 42–55.

7. S. C. Kuo and M. P. Sheetz, Force of single kinesin molecules measured with optical tweezers, *Science* **260** (1993) 232–234.
8. R. J. Hopkins, L. Mitchem, A. D. Ward and J. P. Reid, Control and characterisation of a single aerosol droplet in a single-beam gradient-force optical trap, *Phys. Chem. Chem. Phys.* **6** (2004) 4924–4927.
9. H. Yu, H. Li, Y. Wang, L. Cui, S. Liu and J. Yang, Brief review on pulse laser propulsion, *Opt. Laser Technol.* **100** (2018) 57–74.
10. L. N. Myrabo, M. Libeau, E. Meloney, R. Bracken and T. Knowles, Pulsed laser propulsion performance of 11-cm parabolic bell engines within the atmosphere, in *High-Power Laser Ablation V* (International Society for Optics and Photonics, 2004), pp. 450–464.
11. T. Yabe, C. Phipps, M. Yamaguchi, R. Nakagawa, K. Aoki, H. Mine, Y. Ogata, C. Baasandash, M. Nakagawa and E. Fujiwara, Microairplane propelled by laser driven exotic target, *Appl. Phys. Lett.* **80** (2002) 4318–4320.
12. Z.-Y. Zheng, J. Zhang, Z.-Q. Hao, Z. Zhang, M. Chen, X. Lu, Z.-H. Wang and Z.-Y. Wei, Paper airplane propelled by laser plasma channels generated by femtosecond laser pulses in air, *Opt. Express* **13** (2005) 10616–10621.
13. C. B. Dane, L. A. Hackel, J. Daly and J. Harrison, *Laser Peening of Metals-enabling Laser Technology* (Lawrence Livermore National Laboratory, CA, USA, 1997).
14. A. K. Gujba and M. Medraj, Laser peening process and its impact on materials properties in comparison with shot peening and ultrasonic impact peening, *Materials* **7** (2014) 7925–7974.
15. S. Zou, Z. Cao, Y. Zhao and M. Qian, Laser peening of aluminum alloy 7050 with fastener holes, *Chin. Opt. Lett.* **6** (2008) 116–119.
16. J. Lee and K. Watkins, Removal of small particles on silicon wafer by laser-induced airborne plasma shock waves, *J. Appl. Phys.* **89** (2001) 6496–6500.
17. D. Kim, B. Oh, D. Jang, J.-W. Lee and J.-M. Lee, Experimental and theoretical analysis of the laser shock cleaning process for nanoscale particle removal, *Appl. Surf. Sci.* **253** (2007) 8322–8327.
18. L. Berthe, M. Arrigoni, M. Boustie, J. Cuq-Lelandais, C. Broussillou, G. Fabre, M. Jeandin, V. Guipont and M. Nivard, State-of-the-art laser adhesion test (LASAT), *Nondestruct. Test. Eval.* **26** (2011) 303–317.
19. R. R. Gattass and E. Mazur, Femtosecond laser micromachining in transparent materials, *Nat. Photonics* **2** (2008) 219–225.
20. D. Du, X. Liu, G. Korn, J. Squier and G. Mourou, Laser-induced breakdown by impact ionization in SiO₂ with pulse widths from 7 ns to 150 fs, *Appl. Phys. Lett.* **64** (1994) 3071–3073.
21. A. P. Joglekar, H.-H. Liu, G. Spooner, E. Meyhöfer, G. Mourou and A. Hunt, A study of the deterministic character of optical damage by femtosecond laser pulses and applications to nanomachining, *Appl. Phys. B* **77** (2003) 25–30.
22. E. G. Gamaly, S. Juodkazis, K. Nishimura, H. Misawa, B. Luther-Davies, L. Hallo, P. Nicolai and V. T. Tikhonchuk, Laser-matter interaction in the bulk of a transparent solid: Confined microexplosion and void formation, *Phys. Rev. B* **73** (2006) 214101.
23. B. Wu, Y. Shin, H. Pakhal, N. Laurendeau and R. Lucht, Modeling and experimental verification of plasmas induced by high-power nanosecond laser-aluminum interactions in air, *Phys. Rev. E* **76** (2007) 026405.
24. V. Menezes, K. Takayama, T. Ohki and J. Gopalan, Laser-ablation-assisted microparticle acceleration for drug delivery, *Appl. Phys. Lett.* **87** (2005) 163504.

25. X. Wu, Z. Duan, H. Song, Y. Wei, X. Wang and C. Huang, Shock pressure induced by glass-confined laser shock peening: Experiments, modeling and simulation, *J. Appl. Phys.* **110** (2011) 053112.
26. G. Amontons, De la resistance cause'e dans les machines (1), *J. Jpn. Soc. Tribologis.* **44** (1999) 229–235.
27. K. Anupam, S. Srirangam, A. Scarpas and C. Kasbergen, Influence of temperature on tire–pavement friction: Analyses, *Transp. Res. Rec.* **2369** (2013) 114–124.
28. G.-Q. Chen, Q.-Y. Shi, Y.-J. Li, Y.-J. Sun, Q.-L. Dai, J.-Y. Jia, Y.-C. Zhu and J.-J. Wu, Computational fluid dynamics studies on heat generation during friction stir welding of aluminum alloy, *Comput. Mater. Sci.* **79** (2013) 540–546.
29. I. Iordanoff, B. B. Said, A. Mezianne and Y. Berthier, Effect of internal friction in the dynamic behavior of aerodynamic foil bearings, *Tribol. Int.* **41** (2008) 387–395.
30. O. Braun and A. Naumovets, Nanotribology: Microscopic mechanisms of friction, *Surf. Sci. Rep.* **60** (2006) 79–158.
31. M. H. Müser, L. Wenning and M. O. Robbins, Simple microscopic theory of Amontons's laws for static friction, *Phys. Rev. Lett.* **86** (2001) 1295.
32. H. Sakai, Y. Orihara, H. Kodashima, A. Matsumura, T. Ohkubo, K. Tsuchiya and M. Abe, Photoinduced reversible change of fluid viscosity, *J. Am. Chem. Soc.* **127** (2005) 13454–13455.
33. D. Berman, A. Erdemir and A. V. Sumant, Few layer graphene to reduce wear and friction on sliding steel surfaces, *Carbon* **54** (2013) 454–459.
34. V. Kumar and I. Hutchings, Reduction of the sliding friction of metals by the application of longitudinal or transverse ultrasonic vibration, *Tribol. Int.* **37** (2004) 833–840.
35. D. Hess and A. Soom, Normal vibrations and friction under harmonic loads: part I—Hertzian contacts, *J. Tribol.* **113** (1991) 80–86.
36. A. S. Abdelrahman, J. Sayeed and M. Z. Youssef, Hyperloop transportation system: Analysis, design, control, and implementation, *IEEE Trans. Ind. Electron.* **65** (2017) 7427–7436.
37. B. Xu, K. Ooti, N. Wong and W. Choi, Experimental investigation of flow friction for liquid flow in microchannels, *Int. Commun. Heat Mass Transf.* **27** (2000) 1165–1176.
38. R. Fabbro, J. Fournier, P. Ballard, D. Devaux and J. Virmont, Physical study of laser-produced plasma in confined geometry, *J. Appl. Phys.* **68** (1990) 775–784.
39. S. Zhu, Y. Lu, M. Hong and X. Chen, Laser ablation of solid substrates in water and ambient air, *J. Appl. Phys.* **89** (2001) 2400–2403.
40. L. Berthe, R. Fabbro, P. Peyre and E. Bartnicki, Wavelength dependent of laser shock-wave generation in the water-confinement regime, *J. Appl. Phys.* **85** (1999) 7552–7555.
41. Z. Zhi-Yuan, Z. Yi, Z. Wei-Gong, L. Xin, L. Yu-Tong and Z. Jie, High coupling efficiency generation in water confined laser plasma propulsion, *Chin. Phys. Lett.* **24** (2007) 501.
42. W. Zhang and Y. L. Yao, Micro scale laser shock processing of metallic components, *J. Manuf. Sci. Eng.* **124** (2002) 369–378.